Journal of Multidisciplinary Engineering Science and Technology (JMEST)
ISSN: 2458-9403
Vol. 10 Issue 2, February - 2023

The Stability Analysis Of A Linearly Mass Stratified Fluid Near A Vertical Impermeable Wall Of Constant Temperature And Mass Flux

Maria Neagu
Manufacturing Engineering Department
"Dunarea de Jos" University of Galati,
Galati, Romania
Maria.Neagu@ugal.ro

***Abstract*—This paper analyses the influence of the heat-mass driven regimes succession on the stability of the boundary layers generated by a constant temperature and mass flux vertical impermeable wall situated in a constant temperature and linearly mass stratified environment (air). Two working methods are used: the numerical modeling using the finite differences method and the linear stability analysis (LSA). The numerical modeling considers both an instantaneous as well as a periodic thermal load at the leading edge of the boundary layer and, in this way, it analyzes the instability characteristics of the system. Two particular parameter sets are considered corresponding to the two possible situations: a heat driven convection regime and a heat-mass driven convection regime succession along the wall. The results show that each of the two particular parameter sets considered here defines convectively unstable systems. A notable difference is the influence done by the buoyancy forces in the energy balance of the disturbance motion.**

Keywords—linear stability analysis; finite differences method; natural convection; convective instability

I. INTRODUCTION

The stability analysis of a boundary layer near a vertical impermeable wall is a classical problem of great interest for the scientific community [1-20]. Applications of this problem in the oceanographic double diffusive convection, the melted materials solidification are only a few examples of practical problems that embedded the fundamental scientific results obtained in the last decades.

This paper is continuing this scientific effort by analyzing the stability of the temperature and concentration boundary layers near a vertical impermeable wall that presents a constant temperature and a constant mass flux of a certain constituent. The wall is embedded in a constant temperature and linearly mass stratified environment.

Previous scientific works [21-23] showed that, according to the system parameters, only two situations are possible: a heat driven convection (HDC) or a succession of heat-mass driven convection (HDC-MDC) regimes to attain the equilibrium state along the wall. For a particular parameters set: Prandtl number, $Pr < 1$, Lewis number, $Le \geq 1$, Smith number, $Sch < 1$, Rayleigh number, Ra, the buoyancy ratio, N and the environment mass stratification, S_C, the factor $M = \left[Ra \cdot S_C \cdot Sch^2\right] / \left[N^3 \cdot Pr \cdot (1+Pr)\right]$ defines the two possible situations: a HDC regime along the wall if $M \geq 1$ or a HDC-MDC regime if $M < 1$ (Fig. 1).

This paper analyses two particular parameter sets in a first attempt to understand the influence of the natural convection regimes on the stability of the system [23]: $Ra = 5000$, $N = 1$, $Le = 1$, $Pr = 0.72$, $S_C = 0.08$ (a HDC regime) and $Ra = 5000$, $N = 5$, $Le = 1$, $Pr = 0.72$, $S_C = 0.04$ (a HDC-MDC regime).

Two numerical methods are used in this study:

- The finite differences method is used to study the evolution of the system on two particular thermal inputs: a single mode perturbation applied near the edge of the wall and an instantaneous perturbation applied at an arbitrary point along the wall.
- The linear stability analysis (LSA) method is used to establish the complex wave number (k) for a real frequency (ω) input.

II. MATHEMATICAL FORMULATION

Fig. 1(a) presents the (x,y) coordinate system that is attached to the leading edge of the vertical wall, a wall that has a constant temperature, T_w, and a constant mass flux, m_w, the (u,v) velocity field and, also, h, the upper limit of the computational domain. The environment has, far from the wall, a constant temperature, T_∞, while the linearly stratified concentration of a certain constituent is $C_{\infty,x} = C_0 + s_C \cdot x$, where s_C is the stratification coefficient, C_0 and $C_{\infty,x}$ are the environment concentrations at $x = 0$ and at an arbitrary abscissa, respectively. Fig. 1(b) and Fig. 1(c) show the dimensionless presentation of the problem for the HDC case (Fig. 1(b)) and the HDC-MDC case (Fig. 1(c)).

The dimensional mass, momentum, energy and species concentration conservation equations [21-23], in the Boussinesq approximation, are:

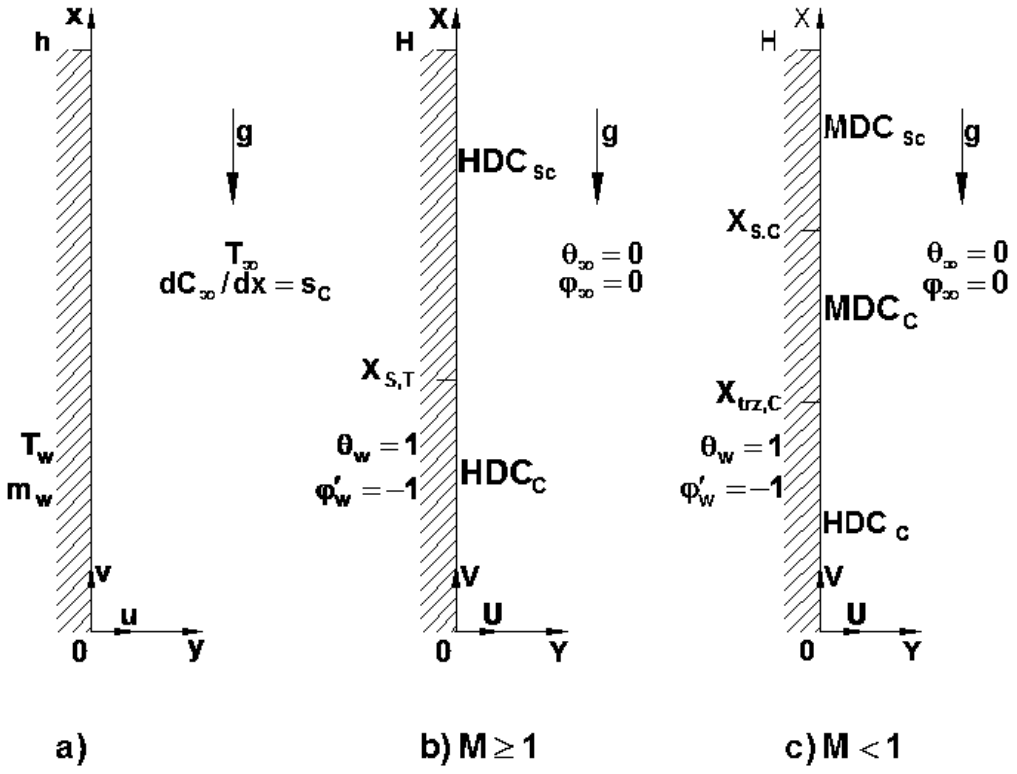

Fig. 1. *(a) The dimensional problem; the dimensionless problem (b) HDC case, (c) HDC-MDC case .*

$$\frac{\partial v}{\partial x}+\frac{\partial u}{\partial y}=0; \quad (1)$$

$$\frac{\partial u}{\partial t}+u\cdot\frac{\partial u}{\partial y}+v\cdot\frac{\partial u}{\partial x}=-\frac{\partial p}{\partial y}+\nu\left(\frac{\partial^2 u}{\partial x^2}+\frac{\partial^2 u}{\partial y^2}\right); \quad (2)$$

$$\frac{\partial v}{\partial t}+u\cdot\frac{\partial v}{\partial y}+v\cdot\frac{\partial v}{\partial x}=$$
$$-\frac{\partial p}{\partial x}+\nu\left(\frac{\partial^2 v}{\partial x^2}+\frac{\partial^2 v}{\partial y^2}\right)+g\beta_t T+g\beta_c C; \quad (3)$$

$$\frac{\partial T}{\partial t}+u\cdot\frac{\partial T}{\partial y}+v\cdot\frac{\partial T}{\partial x}=\alpha\left(\frac{\partial^2 T}{\partial x^2}+\frac{\partial^2 T}{\partial y^2}\right); \quad (4)$$

$$\frac{\partial C}{\partial t}+u\cdot\frac{\partial C}{\partial y}+v\cdot\frac{\partial C}{\partial x}+v\cdot s_c=D\left(\frac{\partial^2 C}{\partial x^2}+\frac{\partial^2 C}{\partial y^2}\right), \quad (5)$$

where α is the thermal diffusivity, D is the mass diffusivity, ν is the kinematic viscosity, T is the temperature field, C is the concentration field, p is the pressure, β_T, is the thermal expansion coefficient, while β_C is the mass expansion coefficient.

The boundary conditions that are applied to the system (1)-(5) are [21-23] -

$$u=v=0,\ T=T_w,\ \frac{\partial C}{\partial y}=-\frac{m_w}{D}\ at\ y=0; \quad (6)$$

$$v=0,\ T=T_\infty,\ C=C_{\infty,x}\ as\ y\to\infty; \quad (7)$$

$$v=0,\ T=T_\infty,\ C=C_{\infty,0}\ at\ x=0; \quad (8)$$

$$\frac{\partial^2 u}{\partial x^2}=\frac{\partial^2 v}{\partial x^2}=\frac{\partial^2 T}{\partial x^2}=\frac{\partial^2 C}{\partial x^2}=0\ at\ x=h. \quad (9)$$

The dimensionless governing equations [21-23]:

$$\zeta=\left(\frac{\partial^2\Psi}{\partial Y^2}+\frac{\partial^2\Psi}{\partial X^2}\right); \quad (10)$$

$$\frac{\partial\zeta}{\partial\tau}+U\frac{\partial\zeta}{\partial Y}+V\frac{\partial\zeta}{\partial X}=$$
$$Pr\cdot\left(\frac{\partial^2\zeta}{\partial Y^2}+\frac{\partial^2\zeta}{\partial X^2}\right)+Ra\cdot Pr\cdot\left(\frac{\partial\theta}{\partial Y}+N\frac{\partial\varphi}{\partial Y}\right); \quad (11)$$

$$\frac{\partial\theta}{\partial\tau}+U\frac{\partial\theta}{\partial Y}+V\frac{\partial\theta}{\partial X}=\frac{\partial^2\theta}{\partial Y^2}+\frac{\partial^2\theta}{\partial X^2}; \quad (12)$$

$$\frac{\partial\varphi}{\partial\tau}+U\frac{\partial\varphi}{\partial Y}+V\frac{\partial\varphi}{\partial X}+VS_C=\frac{1}{Le}\left(\frac{\partial^2\varphi}{\partial Y^2}+\frac{\partial^2\varphi}{\partial X^2}\right), \quad (13)$$

and boundary conditions [21-23]:

$$\Psi = \frac{\partial \Psi}{\partial Y} = 0,\ \frac{\partial \varphi}{\partial Y} = -1,\ \theta = 1 \ at\ Y = 0; \quad (14)$$

$$\frac{\partial \Psi}{\partial Y} = 0,\ \zeta = 0,\ \theta = \varphi = 0 \ as\ Y = L; \quad (15)$$

$$\Psi = 0,\ \zeta = 0,\ \theta = \varphi = 0 \ at\ X = 0; \quad (16)$$

$$\frac{\partial^2 \psi}{\partial X^2} = \frac{\partial^3 \psi}{\partial X^3} = \frac{\partial^2 \theta}{\partial X^2} = \frac{\partial^2 \varphi}{\partial X^2} = 0 \ at\ X = H, \quad (17)$$

are determined by defining the dimensionless coordinates: $X = x/L$, $Y = y/L$, time, $\tau = t\alpha/L^2$, velocity field: $U = u \cdot L/\alpha$, $V = v \cdot L/\alpha$ temperature, $\theta = T - T_\infty / T_w - T_\infty$, concentration, $\varphi = C - C_{\infty,x} / m_w L \cdot D^{-1}$, stratification parameter, $S_C = s_C / (m_W / D)$, stream function: $U = -\partial\Psi/\partial X$; $V = \partial\Psi/\partial Y$, and vorticity, $\zeta = \partial V/\partial Y - \partial U/\partial X$, as well as the Pradtl, $Pr = \nu/\alpha$, Lewis, $Le = \alpha/D$, Smith, $Sch = \nu/D$ and Rayleigh, $Ra = g\beta_t L^3/(\alpha\nu)$, numbers and the buoyancy ratio, $N = \beta_c (m_w/D) L/\beta_t$, where L is the reference length.

III. The Perturbation Regime

In order to analyze the stability of the system a small perturbation is applied to the equilibrium base:

$$\zeta = \zeta_B + \varepsilon \cdot \zeta_D; \quad (18)$$

$$\theta = \theta_B + \varepsilon \cdot \theta_D; \quad (19)$$

$$\varphi = \varphi_B + \varepsilon \cdot \varphi_D; \quad (20)$$

$$\Psi = \Psi_B + \varepsilon \cdot \Psi_D, \quad (21)$$

where the subscripts B and D refer to the base and the perturbation fields, while $\varepsilon << 1$. The system (10)-(13) along with the boundary conditions (14)-(17) are satisfied by the total variables as well as by the base solution. Subsequently, we obtain the dimensionless conservation equations of the perturbation field:

$$\zeta_D = \left(\frac{\partial^2 \Psi_D}{\partial Y^2} + \frac{\partial^2 \Psi_D}{\partial X^2} \right); \quad (22)$$

$$\frac{\partial \zeta_D}{\partial \tau} + (U_B + \varepsilon U_D)\frac{\partial \zeta_D}{\partial Y} + U_D \frac{\partial \zeta_B}{\partial Y} + (V_B + \varepsilon V_D)\frac{\partial \zeta_D}{\partial X} + V_D \frac{\partial \zeta_B}{\partial X} = Pr \cdot \left(\frac{\partial^2 \zeta_D}{\partial Y^2} + \frac{\partial^2 \zeta_D}{\partial X^2} \right) + Ra \cdot Pr \cdot \left(\frac{\partial \theta_D}{\partial Y} + N \frac{\partial \varphi_D}{\partial Y} \right);$$

(23)

$$\frac{\partial \theta_D}{\partial \tau} + (U_B + \varepsilon U_D)\frac{\partial \theta_D}{\partial Y} + U_D \frac{\partial \theta_B}{\partial Y} + (V_B + \varepsilon V_D)\frac{\partial \theta_D}{\partial X} + V_D \frac{\partial \theta_B}{\partial X} = \frac{\partial^2 \theta_D}{\partial Y^2} + \frac{\partial^2 \theta_D}{\partial X^2};$$

$$\frac{\partial \varphi_D}{\partial \tau} + (U_B + \varepsilon U_D)\frac{\partial \varphi_D}{\partial Y} + U_D \frac{\partial \varphi_B}{\partial Y} + (V_B + \varepsilon V_D)\frac{\partial \varphi_D}{\partial X} + V_D \frac{\partial \varphi_B}{\partial X} + V_D S_C = \frac{1}{Le}\left(\frac{\partial^2 \varphi_D}{\partial Y^2} + \frac{\partial^2 \varphi_D}{\partial X^2} \right).$$

(25)

Some scientific researches neglect the εU_D and the εV_D terms of (23)-(25) [1], while other researchers consider the complete form of the disturbance governing equations [2, 4, 6, 7, 14]. Further, this paper neglects the above mentioned terms.

The dimensionless boundary conditions of the perturbation field take the following form:

$$\Psi_D = \frac{\partial \Psi_D}{\partial Y} = 0,\ \varphi_D = \theta_D = 0 \ \text{at}\ Y = 0; \quad (26)$$

$$\frac{\partial \Psi_D}{\partial Y} = 0,\ \zeta_D = 0,\ \theta_D = \varphi_D = 0 \ \text{as}\ Y = L; \quad (27)$$

$$\Psi_D = 0,\ \zeta_D = 0,\ \theta_D = \varphi_D = 0 \ \text{at}\ X = 0; \quad (28)$$

$$\frac{\partial^2 \psi_D}{\partial X^2} = \frac{\partial^3 \psi_D}{\partial X^3} = \frac{\partial^2 \theta_D}{\partial X^2} = \frac{\partial^2 \varphi_D}{\partial X^2} = 0 \ \text{at}\ X = H.$$

(29)

Two perturbation types are applied to the base equilibrium temperature fields.

- An initial, instantaneous perturbation is applied at a certain abscissa along the wall and, then, (30) is imposed at that particular abscissa.

$$\theta_D = A \ \text{at}\ Y = 0 \ \text{and}\ \tau = 0; \quad (30)$$

- A single mode perturbation is applied at the leading edge of the wall, a case when (31) is applied at $X \le 0.05$.

$$\theta_D = A \cdot sin(\omega\tau) \ \text{at}\ Y = 0,\ \tau \ge 0. \quad (31)$$

The governing equations of the perturbation field are solved using the finite differences method. The method as well as the computational domain, number of discretization points and the convergence conditions were described elsewhere [21].

In order to avoid the reflection of the waves at the

upper boundary, a buffer region is considered [2, 4, 7, 19]. Starting at the 0.9H abscissa, at each time step, the buffer region modifies the vorticity as follows [4]:

$$\zeta^{new} = F(X)\cdot\zeta^{old}, \tag{32}$$

where: $F(X) = 1-10\gamma^3+15\gamma^4-6\gamma^5$,
$\gamma = (X-X_{b1})/(X_{b2}-X_{b1})$, $X_{b2} = H$ and $X_{b1} = 0.9H$.

IV. Linear Stability Analysis

This method is completing the method presented above. It gives us a validation of the results obtained using the finite differences method and it helps us to gain insights regarding the mechanisms of the energy balance of the disturbance motion.

A transverse wave is considered along the wall with a complex wave number, k, and a real frequency, ω:

$$\Psi_D = \Pi(Y)e^{i(kx-\varpi\tau)}; \tag{33}$$

$$\theta_D = \Theta(Y)e^{i(kx-\varpi\tau)}; \tag{34}$$

$$\varphi_D = \Phi(Y)e^{i(kx-\varpi\tau)} \tag{35}$$

The horizontal and the vertical velocity field and the vorticity become:

$$U_D = -\frac{\partial\Psi}{\partial X} = -(ik)\Pi e^{i(kX-\omega\tau)} \tag{36}$$

$$V_D = \frac{\partial\Psi}{\partial Y} = \Pi' e^{i(kX-\omega\tau)}; \tag{37}$$

$$\zeta_D = (\Pi''-k^2\Pi)e^{i(kX-\omega\tau)} \tag{38}$$

Replacing (33)-(38) in (22)-(25) and neglecting the higher order products of the perturbation variables, the following system of equations is obtained:

$$Pr\cdot\Pi'''' - U_B\Pi''' + \Pi''\left[-2k^2\,Pr - ikV_B + i\varpi\right] + \Pi'\left[-\frac{\partial\zeta_B}{\partial Y} + k^2U_B\right] + \Pi\left[k^4\,Pr - ik\frac{\partial\zeta_B}{\partial Y} + ik^3V_B - i\varpi k^2\right] + Ra\cdot Pr\cdot\Theta_D' + Ra\cdot N\cdot Pr\cdot\Phi_D' = 0 \tag{39}$$

$$\Theta'' - U_B\,\Theta' + \Theta\left[-k^2 - ikV_B + i\varpi\right] - \Pi'\frac{\partial\theta_B}{\partial X} + ik\Pi\frac{\partial\theta_B}{\partial Y} = 0 \tag{40}$$

$$\frac{1}{Le}\Phi'' - U_B\,\Phi' + \Phi\left[-\frac{1}{Le}k^2 - ikV_B + i\varpi\right] - \Pi'\frac{\partial\varphi_B}{\partial X} - \Pi' S_C + ik\Pi\frac{\partial\varphi_B}{\partial Y} = 0 \tag{41}$$

, where Φ, Π and k are complex numbers.

The boundary conditions applied to the system of equations (39)-(41) are:

$$\Theta = \Phi = \Pi = \Pi' = 0 \text{ at } y = 0; \tag{42}$$

$$\Theta = \Phi = \Pi = \Pi' = 0 \text{ as } y \to \infty. \tag{43}$$

The system (39)-(41) with the associated boundary conditions are solved using the finite differences method with the same characteristics mentioned in [23]. In order to avoid the null solution, the determinant of the matrix obtained after the discretisation must be zero. An iterative process is used in order to find the complex wave number, k, that assures a non-zero solution. The iterative process stops when the absolute value of the determinant is smaller than 1.0e-6 and the square of the norm of the wave number variation is smaller than 1.0e-12.

Previous scientific results [1, 8, 10, 20] show us the way in which the analysis of the conservation equations reveals the rate of change of the kinetic energy through the viscous dissipation, the buoyancy forces and the energy transfer from the base field to the perturbation field for the neutral stability case (the case where k and ω are real numbers). Following their guidance, the dimensionless form of "the energy balance of the disturbance motion" [20], for a complex wave number, $k = k_r + i\cdot k_i$, can be written as follows:

$$\frac{D}{D\tau}KE = -D_M + B + C_M + M_M, \tag{44}$$

or

$$\frac{D}{D\tau}KE = \int_0^{\infty}\int_0^{\lambda}\left[-U_D\cdot V_D\cdot\left(\frac{\partial V_B}{\partial Y}+\frac{\partial U_B}{\partial X}\right) + Ra\cdot Pr\cdot(\Theta_D + N\cdot\Phi_D) - Pr\cdot\left(\frac{\partial U_D}{\partial X}-\frac{\partial V_D}{\partial Y}\right)^2\right]dX\,dY. \tag{45}$$

In (44) and (45) all the terms are real numbers [20]:

$$Re(U_D) = \left[\Pi'_r\cos(\alpha_r X-\omega\tau) + \Pi'_i\sin(\alpha_r X-\omega\tau)\right]e^{-\alpha_i\xi}; \tag{46}$$

$$Re(V_D) = \left[(\Pi_r k_r + \Pi_i k_i)\sin(\alpha_r X-\omega\tau) - (\Pi_i k_r - \Pi_r k_i)\cos(\alpha_r X-\omega\tau)\right]e^{-\alpha_i\xi} \tag{47}$$

The left term of (44) gives us "the rate of change of the disturbance kinetic energy" [20]; D_M is the rate of viscous dissipation; B and C_M are "the rate gain of disturbance kinetic energy through the action of the streamwise buoyancy forces" [20] due to temperature and the concentration fields, respectively; M_M is "the rate of transfer of kinetic energy from the mean flow" [20]:

$$B = \int_0^{\infty} Re\left(\Pi'^{*}\Theta\right)\cdot\frac{Ra\cdot Pr}{4k_i}W\cdot dY \;; \qquad (48)$$

$$C_M = \int_0^{\infty} Re\left(\Pi'^{*}\Phi\right)\frac{Ra\cdot N\cdot Pr}{4k_i}W\cdot dY \;; \qquad (49)$$

$$D_M = \int_0^{\infty}\left|k^2\Pi-\Pi''\right|^2\cdot\frac{Pr}{4k_i}W\cdot V_B\,dY \;; \qquad (50)$$

$$M_M = \int_0^{\infty} Im\left[\Pi'^{*}\cdot\left(\Pi\cdot k^{*}\right)\right]\frac{1}{4k_i}W\cdot dY\,; \qquad (51)$$

$$KE = \int_0^{\infty}\left(\left|\Pi'\right|^2+\left|k\right|^2\left|\Pi\right|^2\right)\frac{1}{4k_i}W\cdot dY\,, \qquad (52)$$

where $W=\left[1-\exp(-4\pi k_r k_i)\right]$, *Re* is the real part and *Im* is the imaginary part of a variable, while * is the complex conjugate variable.

V. RESULTS AND DISCUSSIONS

The first perturbation considered in this analysis is an initial instantaneous thermal load, $\theta = 8$, that is applied at the $X = 3$ abscissa for the HDC case and at the $X = 4$ abscissa for the HDC-MDC case.

Fig. 2 shows the temperature (Fig. 2a) and the concentration (Fig. 2b) perturbation fields at the dimensionless time $\tau = 0.09$ for the HDC case, while Fig. 3 shows the temperature (Fig. 3a) and the concentration (Fig. 3b) perturbation fields at the dimensionless time $\tau = 0.225$ for the HDC-MDc case.

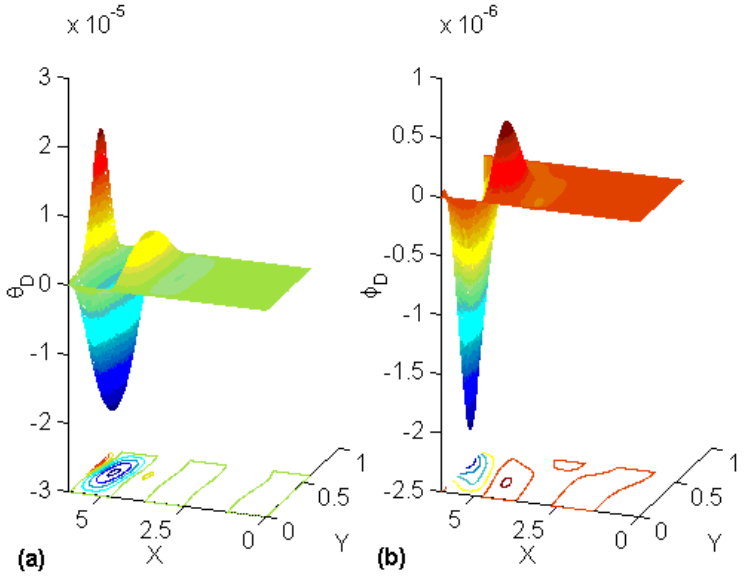

Fig. 2. *Temperature (a) and concentration (b) perturbation field for an instantaneous perturbation at* $X = 3$; $\tau = 0.09$; $A = 8$; $Ra = 5000$, $N = 1$, $Le = 1$, $Pr = 0.72$ and $S_C = 0.08$.

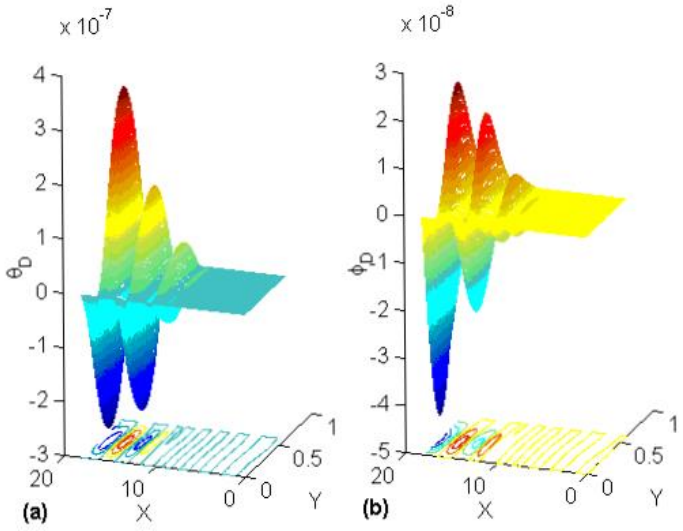

Fig. 3. *Temperature (a) and concentration (b) perturbation field for an instantaneous perturbation at* $X = 4$; $\tau = 0.225$; $A = 8$; $Ra = 5000$, $N = 5$, $Le = 1$, $Pr = 0.72$ and $S_C = 0.04$.

The perturbation moves downstream in both figures proving the presence of a convectively unstable (CU) regime. We conclude that the imaginary part of ω obeys the inequality $\omega_i \le 0$. In this research study only real frequencies, ω, will be considered.

The second type (the single mode) perturbation gives us the possibility to measure the complex wave number of the perturbation field that installs itself in the system for a certain frequency input (ω).

The HDC case is used as a verification of the working method: the frequency of the perturbation input has a value of $\omega = 128.79$. Fig. 4 presents the temperature (Fig. 4(a)) and the concentration (Fig. 4(b)) fields, while Fig. 4(c) and Fig. 4(d) show the time evolution of the temperature and the concentration, for two points: (1.0, 0.2) and (2.0, 0.2). We notice than both the temperature and the concentration values decrease downstream in Fig. 4(a) and Fig. 4(b) revealing a positive spatial growth rate, k_i. From the time evolutions of Fig. 4(c) and Fig. 4(d) we also notice that the temperature and the concentration values have oscillatory behavior and, in time, their amplitude attain the equilibrium value.

For the temperature field, at $y = 0.1$, the calculated medium wave number is $k = 3.73 + i \cdot 1.94$. For the same characteristics, the LSA method gives us a wave number of $k = 3.66 + i \cdot 1.98$ which is a good agreement between the two working methods.

These results show us that the LSA method can be used to determine the complex wave number and to proceed further investigating the behavior of the two cases considered in this paper (the HDC and the HDC-MDC cases).

Further, the LSA method used the following input perturbation frequencies:

- For the HDC case the frequency suggested by the scientific literature [7, 17] for a constant temperature wall is $f = \nu^{-1/3} B(g\beta\Delta T)^{2/3} / 2\pi$, where $B = 0.315 \cdot Pr^{-0.065}$. Consequently, the frequency $\omega = 0.2884 \cdot Ra^{2/3} = 84.3405$. The LSA analysis determines a complex wave number of $k = 2.562 + i \cdot 1.639$.
- For the HDC-MDC case, the frequency suggested by the scientific literature [17] for a constant heat flux at the wall is $f^* = B^* (g\beta q'' / k)^{2/3} / 2\pi$, where $B^* = 1.04 \cdot Pr^{-1/4}$. Consequently, the frequency $\omega = 0.958 \cdot Ra^{1/2} = 67.7410$. The LSA analysis gives us a value of $k = 1.86 + i \cdot 0.92$.

Fig. 5 presents the results of the LSA method.

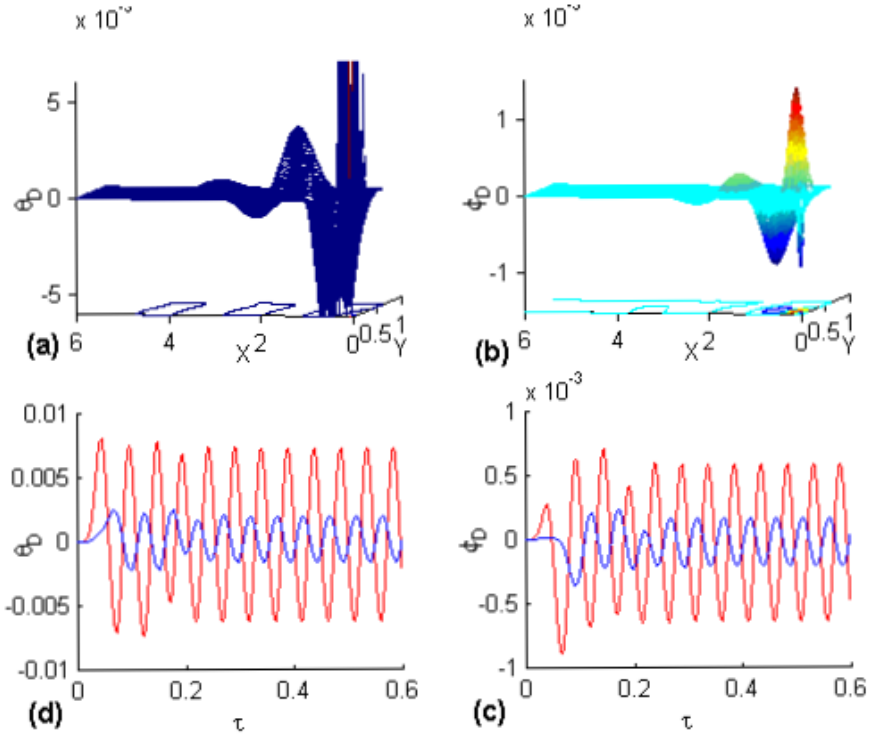

Fig. 4. *Temperature (a), concentration (b) perturbation fields at* $\tau = 0.6018$ *; temperature (c) and concentration (d) time variation at two points:* $(1.0,0.2)$*—red line and* $(2.0,0.2)$*—blue line; the thermal load is* $\theta = 8\sin(\omega\tau)$*,* $\omega = 128.7941$ *for* $X < 0.05$, $Y = 0$, $\tau \ge 0$; $Ra = 5000$, $N = 1$, $Le = 1$, $Pr = 0.72$ *and* $S_C = 0.08$.

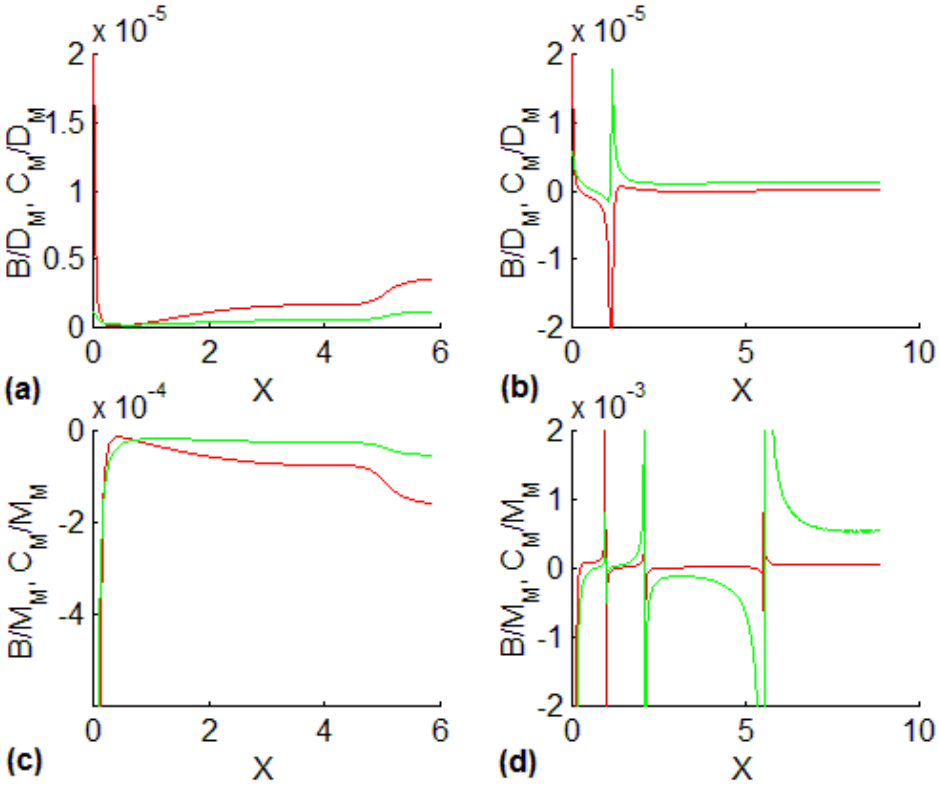

Fig. 5. *B/D_M (red line) and C_M/D_M (green line) ratio variation for the HDC case (a) and the HDC-MDC case (b); B/M_M (red line) and C_M/M_M (green line) ratio variation for the HDC case (c) and the HDC-MDC case (d).*

Fig. 5(a) presents the evolution of the B/D_M (the "relative buoyant production" [10]) and C_M/D_M ratios along the wall for the HDC case. For this case both ratios have positive values indicating a destabilizing effect of the buoyancy forces. Fig. 5(a) shows that, in this case, the contribution of the buoyancy forces, B and C_M, is smaller than the contribution of the viscous dissipative term, D_M, to the energy balance of the disturbance motion. We notice that the thermal buoyancy forces have a greater contribution that the buoyancy forces due to the presence of the constituent.

Fig. 5(b) shows the evolution of the B/D_M and C_M/D_M ratios along the wall for the HDC-MDC case. Both ratios have a destabilizing effect on the perturbation flow, but the D_M values are always bigger than the B or C_M values. We, also, notice that for the HDC-MDC case the thermal buoyancy contribution to the perturbation flow is, in general, smaller than the contribution due to the concentration field. A special attention can be given to the $X = 1.2$ abscissa where strong negative values are encountered for the B/D_M ratio, while the C_M/D_M ratio has a relatively high positive value. As a transition from a heat driven convection to a mass driven convection is expected to take place at the point on the wall with an $X = 3.34$ abscissa, we can expect that this transition is the cause of the opposing tendencies of the two types of buoyancy forces. Further studies should analyze this aspect.

Fig. 5(c) presents the B/M_M and the C_M/M_M ratios variation along the wall for the HDC case. We notice the negative values of M_M for this particular parameter set and the small values of both B/M_M and C_M/M_M ratios. It is clear that the "Reynolds stress term", M_M [20], is taking energy from the disturbance flow and its values are much higher that the energy added to the perturbation flow by the buoyancy forces.

Fig. 5(d) shows the evolution of the B/M_M and the C_M/M_M ratios along the wall for the HDC-MDC case. The ratios have negative and positive values alternating along the wall. Two points are of great interest in this case [23]: the $X = 3.34$ point, where heat-mass driven change takes place in the base flow and the abscissa $X = 7.73$ where the $\partial C/\partial x > s_C$ in (5). This result invites to a deeper analysis of the energy balance of the disturbance motion for a clearer understanding of this complex variation.

VI. Conclusions

This paper is an analysis of the stability of two natural convection regimes:

- a HDC regime with the following characteristics: $Ra = 5000$, $N = 1$, $Le = 1$, $Pr = 0.72$ and $S_C = 0.08$.
- a HDC-MDC natural convective regime with: $Ra = 5000$, $N = 5$, $Le = 1$, $Pr = 0.72$ and $S_C = 0.04$.

These two regimes are convectively unstable as an instantaneous perturbation initiated at an arbitrary abscissa of the wall moves downstream.

The buoyancy forces due to both temperature and concentration are destabilizing the system in both cases but, for the HDC regime the temperature buoyancy forces have a greater influence than the concentration buoyancy force, while for the second case the reverse is true. The work done by the buoyancy forces are always smaller than both the rate of viscous dissipation and the rate of kinematic energy transferred from or to the perturbation flow.

This analysis is a first step toward the complete understanding of the influence that the heat/mass driven natural convection regime succession can have on the stability of this system. Further analysis for higher values of Rayleigh numbers should be considered. Also, studies on the resonance frequencies of these systems could be a subject of great scientific interest.

REFERENCES

[1] A. E. Gill and A. Davey, "Instabilities of a buoyancy-driven system," Journal of Fluid Mechanics, vol. 35 (4), 1969, pp. 775-798.

[2] T. Aberra, S. W. Armfield, M. Behnia and G. D. McBain, "Boundary layer instability of the natural convection flow on a uniformly heated vertical plate," International Journal of Heat and Mass Transfer, vol. 55, 2012, pp. 6097-6108.

[3] M. C. Paul, D .A. S. Rees and M. Wilson, "The influence of higher order effects on the linear wave instability of vertical free convective boundary layer flow," International Journal of Heat and Mass Transfer , vol. 48, 2005, pp. 809-817.

[4] M. C. Paul, D. A. S. Rees and M. Wilson, "Thermal receptivity of free convective flow from a heated vertical surface: Linear waves," International Journal of Thermal Sciences, vol. 47, 2008, pp. 1382-1392.

[5] M. Gaster, "A note on the relation between temporally-increasing and spatially-increasing disturbances in hydrodynamic stability," Journal of Fluid Mechanics, vol. 14, 1962, pp. 222-224.

[6] Y. Zhao, P. Zhao, Y. Liu, Y. Xu and J. F. Torres, "On the selection of perturbations for thermal boundary layer control," Physics of Fluids, vol. 31, 2019, pp. 1-14.

[7] Y. Zhao, C. Lei and J. C. Patterson, "Resonance of the thermal boundary layer adjacent to an isothermally heated vertical surface," Journal of Fluid Mechanics, vol. 724, 2013, pp. 305-336.

[8] P. A. Iyer, "Instabilities in buoyancy-driven boundary-layer flows in a stably stratified medium," Boundary-Layer Meteorology, vol. 5, 1973, pp. 53-66.

[9] Y. Zhao, C. Lei and J. C. Patterson, "Natural transition in natural convection boundary layers," International Communications in Heat and Mass Transfer, vol. 76, 2016, pp. 366-375.

[10] G. D. McBain, S. W. Armfield and G. Desrayaud, "Instability of the buoyancy layer on an evenly heated vertical wall," Journal of Fluid Mechanics, vol. 587, 2007, pp. 453-469.

[11] Y. Zhao, C. Lei and J. C. Patterson, "Transition of natural convection boundary layers — a revisit by Bicoherence analysis," International Communications in Heat and Mass Transfer, vol. 58, 2014, pp. 147-155.

[12] J. Tao, P. Le Quéré and S. Xin, "Absolute and convective instabilities of natural convection flow in boundary-layer regime," Physical Review E, vol. 70, 066311, 2004, pp. 1-7.

[13] J. Tao, P. Le Quéré and S. Xin, "Spatio temporal instability of the natural-convection boundary layer in thermally stratified medium," Journal of Fluid Mechanics, vol. 518, 2004, pp. 363-379.

[14] J. Tao, "Nonlinear global instability in buoyancy driven boundary-layer flows," Journal of Fluid Mechanics, vol. 566, 2006, pp. 377-388.

[15] A. A. Szewczyk, "Stability and transition of the free-convection layer along a vertical flat plate," International Journal of Heat and Mass Transfer, vol. 5, 1962, pp. 903-914.

[16] K. Venkatasubbaiah and T. K. Sengupta, "Mixed convection flow past a vertical plate: Stability analysis and its direct simulation," International Journal of Thermal Sciences, vol. 48, 2009, pp. 461-474.

[17] B. Gebhart and E. Mahajan, "Characteristic disturbance frequency in vertical natural convection flow," International Journal of Heat and Mass Transfer, vol. 18, 1975, pp. 1143-1148.

[18] L. Krizhevsky, J. Cohen and J. Tanny, "Convective and absolute instabilities of a buoyancy-induced flow in a thermally stratified medium," Physics of Fluids, vol. 8, 1996, pp. 971-977.

[19] M. Kloker, U. Konzelmann and H. Fasel, "Outflow boundary conditions for spatial Navier-Stokes simulations of transition boundary layers," AAIA Journal, vol. 31, 1993, pp. 620-628.

[20] P. R. Nachtsheim, "Stability of free-convection boundary-layer flows," NASA TN D-2089, 1963.

[21] M. Neagu, "Natural convection near a vertical wall of constant mass flux and temperature situated in a mass stratified fluid," IOP Conference Series: Materials Science and Engineering, vol. 444, 2018, pp. 1–14.

[22] M. Neagu, "Heat/mass driven natural convection of air near a boundary of constant mass flux and temperature," Journal of Multidisciplinary Engineering Science and Technology, vol. 8, 2021, pp. 14727-14735.

[23] M. Neagu, "The Succession of Heat and Mass Driven Natural Convection Regimes Along a Vertical Impermeable Wall," European Journal of Natural Sciences and Medicine, vol. 5, 2022, pp. 9-26.